BUCKLING ANALYSIS OF VARIABLE ANGLE TOW COMPOSITE PLATES WITH ONE CIRCULAR DELAMINATION

Zhangming Wu[1*], Xiaodong Chen[2] and Paul. M. Weaver[3]

[1] Cardiff School of Engineering, Cardiff University, UK wuz12@cardiff.ac.uk
[2] School of Aerospace Engineering and Applied Mechanics, Tongji University, China
[3] ACCIS, Department of Aerospace Engineering, QB, University of Bristol, UK

Keywords: Composite Plates, Buckling, Delamination, Variable Angle Tow, Variable Stiffness

ABSTRACT

Advanced carbon-fibre composite materials are increasingly used as primary structural components in aviation and aerospace industries due to their high stiffness-to-density ratio. The design of composite aerostructures is required to meet a number of safety criteria, in particular, the damage tolerance. Delaminations, which are caused by the impact of foreign objects (tool drops, runway debris, bird strikes etc) or the manufacture process, are one of the most common damage defects of laminated composite structures. The delaminations may lead to the occurrence of the local buckling and/or the global buckling before the ultimate design load, and therefore reduce the load-carrying capacity of composite structures. The mechanics of laminated composite structures containing delaminations had been extensively studied by many researchers in last two decades. With an increased understanding of the failure mechanism due to the delaminations, the damage tolerance constraints can be considered in the optimal design of composite structures. However, a finite element method using the cohesive elements or the Virtual Crack Closure Technique (VCCT) is normally very time-consuming to perform the damage analysis of composite laminates. Therefore, developing an analytical modelling to compute the residual buckling or postbuckling strength after the delaminations remains importance, not only for the availability of an efficient design tool but also for the study of physical insights of delaminations. A number of previous works had applied the analytical modelling to study the effect of a delamination or delaminations on buckling and postbuckling strength of constant stiffness composite plates. This work developed a Rayleigh-Ritz modelling to analyse the buckling behaviour of VAT plates with one circular delamination. Taking advantages of the advanced VAT laminates to improve the damage tolerance of composite structures remains great potential. However, the damage mechanics and the failure mechanism of VAT composite laminates containing delaminations have never been well studied. This work performed the parametric study of the compressive buckling load of the VAT laminates with linear variation of fibre angles. The results reveal the benefits of utilizing the variable stiffness tailoring to improve the delaminated buckling resistance of composite structures.

1 INTRODUCTION

Recently, the advanced tow-steering technology enables us to design and manufacture the variable angle tow (VAT) composite laminates [1-8], in which the fibre orientation angles are allowed to continuously vary across the plane of composite plies. The VAT concept offers the designers very large design flexibility due to their variable stiffness properties. A number of previous works had shown that the VAT laminates can significantly increase the buckling and postbuckling load-carrying capacity of composite structures. Taking advantages of the advanced VAT laminates to improve the damage tolerance of composite structures remains great potential. This work develops an efficient analytical modelling to study the compressive buckling behaviour of the VAT laminates with an embedded circular delamination. The mechanism of utilizing the tow-steering technology to improve the residual buckling strength of delaminated composite plates is then analysed based on the results obtained from a parametric study.

In the present work, a Rayleigh-Ritz modelling is developed to analyze the buckling performance of VAT panels with embedded delaminations under uniform displacement axial compression. For the sake of simplicity, only a 1/2 depth located circular delamination is considered in our initial study. The analytical modelling is derived based on the minimum principle of potential energy (or complementary energy) and an assumption of equally spaced delaminations. This assumption allows us to avoid considering the delamination opening and contact problems, which are barely observed in the previous experimental testing [citations]. The prebuckling analysis of the delaminated VAT panels is identical to the previous work developed for the intact VAT panels, in which a double series expansion of the Airy's stress function is applied to capture the highly non-uniform stress distributions. For the buckling analysis, the superposition method with local shape functions is applied to model the local buckling behaviour of the delamination area. Additional terms are also introduced to ensure the continuity of in-plain displacements and strains along the boundary of the circular delamination region. Both the global and local shape functions are constructed using the Legendre polynomials instead of double sine series, which enable the accurate simulation of the delamination buckling behaviour of VAT panels with highly anisotropic bending-twisting coupling. This analytical method is capable to capture both the local buckling shape of the delaminated sublaminate and the global buckling mode of the whole VAT panel. The major difficulties for this analytical modelling lies in the circular delamination boundary and the increased bending-twisting coupling of sublaminates. To verify the proposed method, results are compared with those obtained using FE simulation performed on ABAQUS commercial software. The accuracy and efficiency of this proposed model are also validated. Subsequently, parametric study on the delamination buckling behaviour of VAT panels with linear variation of fiber orientation angles is carried out. A great amount of results are obtained and used to analyze the benefits given by the tow steering laminates to enhance the delamination buckling performance of composite panels.

2 DELAMINATED VAT LAMINATES

A simply supported rectangular VAT panel with one central located circular delamination under a uniform displacement compressive loading, as shown in Figure. 1, is considered in this work. The delaminated VAT panel is divided into three portions by the middle delamination interface. The undelaminated portion is denoted by *0* and the delaminated portions are then denoted by *sub=1, 2*.

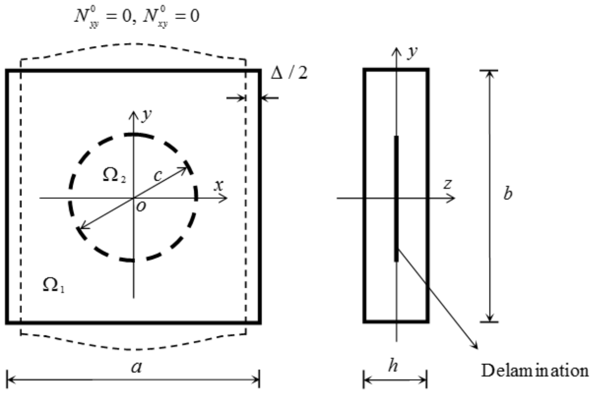

Figure. 1 The geometry and in-plane boundary condition of a VAT panel with a circular delamination

For simplicity, the VAT laminates with no extension-bending coupling (B=0) and no extension-shear coupling (A_{16}=0, A_{26}=0) are studied in this work. Note, the delaminations may violate such reduced coupling effects of VAT laminates. In this work, the VAT panel is constructed with a 16-layer anti-symmetric layup $[\pm\theta_1/\mp\theta_1]_{2As}$, which generally exhibits specially orthotropic properties. Particularly, the sub laminates are still symmetric and balanced with respect to the mid-plane of each portion, when the delaminations occur at the middle interface or equally spaced interfaces. With the B=0, the constitutive equations for each portion of the entire delaminated VAT panel are expressed in the following partially inverted form,

$$\begin{Bmatrix} \varepsilon_{xx}^{L} \\ \varepsilon_{yy}^{L} \\ \varepsilon_{xy}^{L} \\ M_{xx}^{L} \\ M_{yy}^{L} \\ M_{xy}^{0} \end{Bmatrix} = \begin{bmatrix} a_{11}^{L} & a_{12}^{L} & a_{16}^{L} & 0 & 0 & 0 \\ a_{12}^{L} & a_{22}^{L} & a_{26}^{L} & 0 & 0 & 0 \\ a_{16}^{L} & a_{26}^{L} & a_{66}^{L} & 0 & 0 & 0 \\ 0 & 0 & 0 & D_{11}^{L} & D_{12}^{L} & D_{16}^{L} \\ 0 & 0 & 0 & D_{12}^{L} & D_{22}^{L} & D_{26}^{L} \\ 0 & 0 & 0 & D_{16}^{L} & D_{26}^{L} & D_{66}^{L} \end{bmatrix} \begin{Bmatrix} N_{xx}^{L} \\ N_{yy}^{L} \\ N_{xy}^{L} \\ \kappa_{xx}^{L} \\ \kappa_{yy}^{L} \\ \kappa_{xy}^{L} \end{Bmatrix} \quad (L = 0 \text{ or sub}) \qquad (1)$$

where 0 and $\text{sub}(\text{sub}=1,2)$ denote the undelaminated portion and each delaminated portion, respectively. $\varepsilon_{xx}^{L}, \varepsilon_{yy}^{L}, \varepsilon_{xy}^{L}$, $\kappa_{xx}^{L}, \kappa_{yy}^{L}, \kappa_{xy}^{L}$ are mid-plane strains and curvatures of each portion, respectively. $N_{xx}^{L}, N_{yy}^{L}, N_{xy}^{L}$ and $M_{xx}^{L}, M_{yy}^{L}, M_{xy}^{L}$ are in-plane stress and bending moment resultants, respectively. $D_{ij}^{L}(i,j=1,2,6)$ are bending stiffness coefficients; $a_{ij}^{L}(i,j=1,2,6)$ are the in-plane flexural stiffness coefficients. The total bending stiffness of an intact plate with the same layup configuration in the delamination region is approximately four times of that of a delaminated VAT panel. The reduction of bending stiffness in the delamination region is the major reason that leads to the considerable reduction of the buckling strength.

3 THEORETICAL MODELLING

In this work, an analytical modelling based on the Rayleigh-Ritz method is developed to solve the buckling problem of the delaminated VAT plates. The total potential energy Π of the delaminated VAT panel can be obtained, as follows

$$\Pi = U + V \qquad (2)$$

where V denotes the external work of the applied load; U is the strain energy of the VAT panel in its buckled shape and expressed as

$$U = U_{\text{bend.}}^{0} + \sum_{\text{sub}=1}^{2} U_{\text{bend.}}^{\text{sub}} + \sum_{\text{sub}=1}^{2} U_{\text{in-plane}}^{\text{sub}} \qquad (3)$$

where U_{bend}^{0}, $U_{\text{bend}}^{\text{sub}}$ are bending strain energies of the undelaminated portion and each delaminated portion, respectively. $U_{\text{in-plane}}^{\text{sub}}$ is in-plane strain energy for each delaminated portion. Substituting the shape functions of displacements and the prebuckling stress resultants into (2) and minimizing the total potential energy Π with respect to $U_{pq}^{sub}, V_{pq}^{sub}, W_{mn}^{0}$ and $\overline{W}_{\bar{m}\bar{n}}^{sub}$, a set of nonlinear algebraic equations are obtained and expressed in the following matrix form,

$$\left(\begin{bmatrix} \mathbf{K}_{\text{UU}} & \mathbf{K}_{\text{UV}} & \mathbf{K}_{\text{UW}} & \mathbf{0} \\ \mathbf{K}_{\text{VU}} & \mathbf{K}_{\text{VV}} & \mathbf{K}_{\text{VW}} & \mathbf{0} \\ \mathbf{K}_{\text{WU}} & \mathbf{K}_{\text{WV}} & \mathbf{K}_{\text{WW}} & \mathbf{K}_{\text{W}\overline{\text{W}}} \\ \mathbf{0} & \mathbf{0} & \mathbf{K}_{\overline{\text{W}}\text{W}} & \mathbf{K}_{\overline{\text{W}}\overline{\text{W}}} \end{bmatrix} + \lambda \begin{bmatrix} \mathbf{0} & \mathbf{0} & \mathbf{0} & \mathbf{0} \\ \mathbf{0} & \mathbf{0} & \mathbf{0} & \mathbf{0} \\ \mathbf{0} & \mathbf{0} & \mathbf{L}_{\text{WW}} & \mathbf{L}_{\text{W}\overline{\text{W}}} \\ \mathbf{0} & \mathbf{0} & \mathbf{L}_{\overline{\text{W}}\text{W}} & \mathbf{L}_{\overline{\text{W}}\overline{\text{W}}} \end{bmatrix} \right) \begin{Bmatrix} \mathbf{U} \\ \mathbf{V} \\ \mathbf{W} \\ \overline{\mathbf{W}} \end{Bmatrix} = \begin{Bmatrix} \mathbf{0} \\ \mathbf{0} \\ \mathbf{0} \\ \mathbf{0} \end{Bmatrix} \qquad (4)$$

where for example, $\mathbf{K}_{\text{UW}}$ is the factor of the unknown coefficient $\mathbf{U}$ that arises from minimizing the total potential energy with respect to $\mathbf{W}$; $\mathbf{L}_{\text{W}\overline{\text{W}}}$ is the factor of the unknown coefficient $\mathbf{W}$ that arises from minimizing the total potential energy with respect to $\overline{\mathbf{W}}$; λ is the eigenvalue. The in-plane generalized displacements $\mathbf{U}$ and $\mathbf{V}$ are given by

$$\begin{Bmatrix} \mathbf{U} \\ \mathbf{V} \end{Bmatrix} = -\begin{bmatrix} \mathbf{K}_{\text{UU}} & \mathbf{K}_{\text{UV}} \\ \mathbf{K}_{\text{UU}} & \mathbf{K}_{\text{UU}} \end{bmatrix}^{-1} \begin{bmatrix} \mathbf{K}_{\text{UW}} \\ \mathbf{K}_{\text{VW}} \end{bmatrix} \{\mathbf{W}\} \qquad (5)$$

Thus, the reduced equations take the following matrix form,

$$\left(\begin{bmatrix} \overline{\mathbf{K}}_{\mathrm{WW}} + \mathbf{K}_{\mathrm{WW}} & \mathbf{K}_{\mathrm{W}\overline{\mathrm{W}}} \\ \mathbf{K}_{\overline{\mathrm{W}}\mathrm{W}} & \mathbf{K}_{\overline{\mathrm{W}}\overline{\mathrm{W}}} \end{bmatrix} + \lambda \begin{bmatrix} \mathbf{L}_{\mathrm{WW}} & \mathbf{L}_{\mathrm{W}\overline{\mathrm{W}}} \\ \mathbf{L}_{\overline{\mathrm{W}}\mathrm{W}} & \mathbf{L}_{\overline{\mathrm{W}}\overline{\mathrm{W}}} \end{bmatrix}\right) \begin{Bmatrix} \mathbf{W} \\ \overline{\mathbf{W}} \end{Bmatrix} = \begin{Bmatrix} \mathbf{0} \\ \mathbf{0} \end{Bmatrix} \tag{6}$$

where

$$\overline{\mathbf{K}}_{\mathrm{WW}} = -\begin{bmatrix} \mathbf{K}_{\mathrm{WU}} & \mathbf{K}_{\mathrm{WV}} \end{bmatrix} \begin{bmatrix} \mathbf{K}_{\mathrm{UU}} & \mathbf{K}_{\mathrm{UV}} \\ \mathbf{K}_{\mathrm{UU}} & \mathbf{K}_{\mathrm{UU}} \end{bmatrix}^{-1} \begin{bmatrix} \mathbf{K}_{\mathrm{UW}} \\ \mathbf{K}_{\mathrm{VW}} \end{bmatrix} \tag{7}$$

The eigenvalue λ is then obtained by solving the eigenvalue problem of Eq. (42). The lowest eigenvalue λ_{cr} corresponds to the critical buckling displacement to be found.

4 FINITE ELEMENT ANALYSIS

Compressive buckling behavior of a simply-supported VAT laminated panel with a mid-plane located circular delamination is also modelled in the commercial package Abaqus. An additional script was developed to generate the FEM routines for the buckling analysis of VAT panels with delaminations, in which each element is assigned with an independent fiber orientation. Figure 2 illustrates the finite element meshing pattern that divides the VAT panel into three regions with independent mesh sizes. The inner small rectangular plate and the outside circular region define the area where the delamination occurred, and the rest part is the undamaged region. Herein, a three-dimensional, isoparametric and 8-node hexahedron continuum shell element (SC8R) is chosen to model each VAT layer. The thickness direction of SC8R elements is defined with respect to the stacking sequence of VAT laminates. To simulate the delamination effect in the FEM modelling, the VAT panel is split into two individual parts at the interface of delamination. Subsequently, the undamaged region of two parts are tied through the multi-point constraints (MPC).

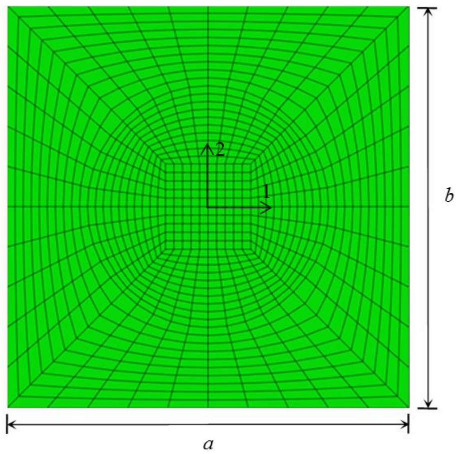

Figure.2 FEM model mesh for a VAT panel with a circular delamination 1/2 depth located

5 RESULTS AND DISCUSSION

Suemasu et al. [20] has shown that the existence of delamination results in considerable loss of the buckling load of a plate containing a delamination due to the decrease of the bending stiffness at the delaminated area. For comparison purposes, three delaminated VAT panels and two delaminated conventional panels are included for buckling analysis: (a) $[90 \pm \langle 30{,}65\rangle]_{4s}$, (b) $[90 \pm \langle 0{,}75\rangle]_{4s}$, (c) $[90 \pm \langle 20{,}90\rangle]_{4s}$, (d) $[0]_{16}$, (e) $[\pm 45]_{4s}$, (f) $[90]_{16}$. Fig. 3 shows the buckling coefficients versus the NDR value of the delaminated panel with the NDR value ranging from 0.0 to 0.7 and the results obtained using Rayleigh-Ritz method and FE simulation are very close to each other. As shown in Fig. 3, it is obviously seen that the buckling performance of the delaminated VAT panels is superior to that of the delaminated conventional panels. From Fig. 3, the plate $[\pm 45]_{16}$ exhibits the maximum buckling coefficient among all conventional plate configurations and the buckling coefficient starts to drop when the NDR value exceeds 0.4. However, the buckling coefficient of the delaminated VAT plate $[90 \pm \langle 20,90 \rangle]_{4s}$ is slightly larger than that of the plate $[\pm 45]_{4s}$ but remains almost unchanged with the increase in the NDR value. The plate $[0]_{16}$ remains almost constant by slight changes in the NDR value but exhibits relatively low buckling performance, while the delaminated VAT plate $[90 \pm \langle 30,65 \rangle]_{4s}$has the relatively high buckling coefficient and only starts to drop around the NDR value 0.5. In addition, the delaminated VAT plate $[90 \pm \langle 0,75 \rangle]_{4s}$ keeps the highest buckling coefficient among all the delaminated panels considered with the NDR value increased. The primary reason for the improvement of the buckling performance of the delaminated VAT panel is that the applied load is redistributed away from the central region of the delaminated VAT panel towards the transverse edges. In so doing, the in-plane stress resultants within the delamination region decreases such that the delaminated VAT panels, despite the presence of the delamination, exhibit enhanced buckling performance.

Fig. 4 shows the buckling coefficients versus the NDR values of all the delaminated VAT plate configurations $[90 \pm \langle T_0, T_1 \rangle]_{4s}$ obtained using the present Rayleigh-Ritz method. In Fig. 4, it is obviously seen that the delaminated VAT panels exhibit more flexibility in stiffness tailoring to achieve better buckling performance compared to the delaminated conventional panels. For most delaminated VAT panels, despite the presence of delamination, the buckling coefficient remains almost unchanged with the increase in the NDR value.

6 CONCLUSIONS

In this paper, an improved Rayleigh-Ritz method is developed for the buckling analysis of the VAT panel with a circular midplane delamination, which is subjected to uniform axial compression. The analytical model is based on the classical laminated plate theory and the assumption that each delaminated portion undergoing the same amount deformation during the buckling process. For the buckling analysis, both global and local shape functions are constructed by Legendre polynomials instead of double sine series, which satisfy both geometric boundary conditions and continuity conditions. Besides, the finite element analysis is performed on ABAQUS commercial software. Results obtained by the proposed method are compared with the FE results and it was observed that the proposed method yield accurate results with less computational effort. The fast convergence, robustness and efficiency of the proposed method are demonstrated.

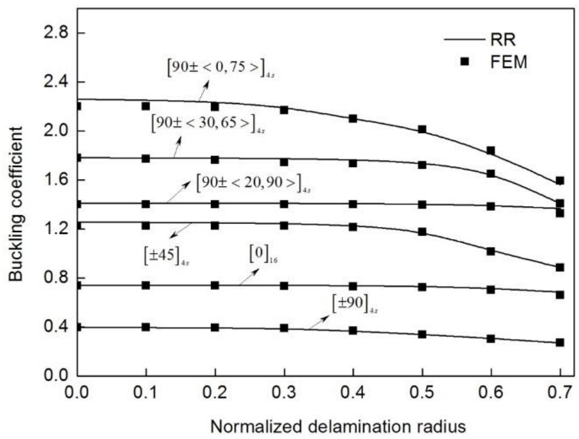

Fig.3 Buckling coefficient vs normalized delamination radius for various VAT and conventional panels with a circular delamination

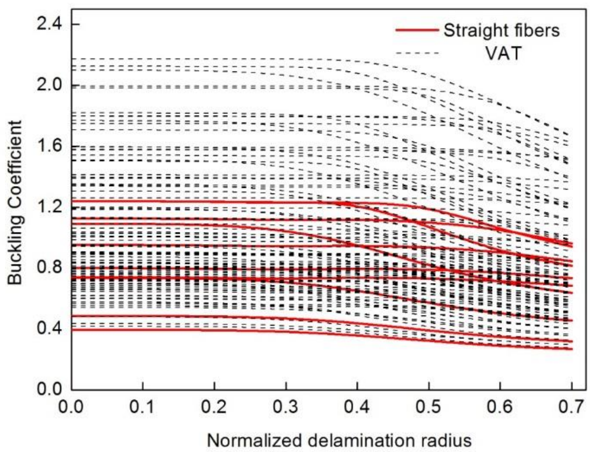

Fig.4 Buckling coefficient vs normalized delamination radius for various VAT panels with a circular delamination 1/2 depth located

ACKNOWLEDGEMENTS

The first author wish to sincerely acknowledge the financial support from China's 1000 Young Talent Programme and the Strathclyde Chancellor's Fellowship (University of Strathclyde, Scotland). Weaver would like to thank SFI (Science Foundation Ireland) for funding under its Research Professor programme.

REFERENCES

[1] Hyer MW, Lee HH. The use of curvilinear fiber format to improve buckling resistance of composite plates with central holes. Compos Structure 1991;18.

[2] Olmedo R, Gurdal Z. Buckling response of laminates with spatially varying fiber orientations. In: Collection of technical papers—AIAA/ASME structures, structural dynamics and materials conference 1993.p.2261–69.

[3] Gurdal Z, Tatting B, Wu C. Variable stiffness composite panels: effects of stiffness variation on the in-plane and buckling response. Composites Part A: Applied Science and Manufacturing 2008; 39(5):911–22.

[4] Setoodeh S, Abdalla M M, IJsselmuiden S T, Gurdal Z. Design of variable stiffness composite panels for maximum buckling load. Composite Structure 2008; 87:109–17.
[5] IJsselmuiden S T, Abdalla M M, Gurdal Z. Optimization of variable-stiffness panels for maximum buckling load using lamination parameters. AIAA Journal 2010; 48(1):134–43.
[6] Wu Z, Weaver P M, Raju G, Kim B C. Buckling analysis and optimization of variable angle tow composite plates. Thin-Walled Structures 2012;60, 163–172.
[7] Raju G, Wu Z, Kim B C, Weaver P M. Prebuckling and buckling analysis of variable angle tow plates with general boundary conditions. Composite Structure 2012; 94: 2961-2970.
[8] Coburn B H, Wu Z, Weaver P M. Buckling analysis of stiffened variable angle tow panels. Composite Structure 2014; 111: 259-270.
[9] Chai H, Babcock C D, Knauss W G. One dimensional modeling of failure in laminated plates by delamination buckling. Int J Solids Struct 1981;17(11):1069–83.
[10] Simitses G J, Sallam S, Yin W L. Effect of delamination of axially loaded homogeneous laminated plates. AIAA Journal 1985;9(23):1437-1444.
[11] Shivakumar K N, Whitcomb J D. Buckling of a sublaminate in a quasi-isotropic composite laminate. Journal of Composite Materials 1985;19:2-18.
[12] Kardomateas G A, Schmueser D W. Buckling and postbuckling of delaminated composites under compressive loads including transverse shear effects. AIAA Journal 1988; 26(3): 337-343.
[13] Lee J, Gurdal Z, Griffin O H. A layerwise approach for the bifurcation problem in laminated composites with delaminations. AIAA Journal 1993; 31(2):331-338.
[14] Shu D. Buckling of multiple delaminated beams. International Journal of Solids and Structures 1998; 35(13):1451-1465.
[15] Kim H, Kedward K T. A method for modeling the local and global buckling of delaminated composites plates. Composite Structure 1999; 44:43-53.
[16] Bruno D, Greco F. An asymptotic analysis of delamination buckling and growth in layered plates. International Journal of Solids and Structures 2000; 37: 6239-6276.
[17] Oversy H R, Kharazi M, Taghizadeh M. Semi-analytical buckling analysis of clamped composite plates containing embedded rectangular and circular delaminations. Mechanics of Advanced Materials and Structures 2010; 17:343-352.
[18] Kharazi M, Oversy H R, Taghizadeh M. Buckling of the composite laminates containing through-the-width delaminations using different plate theories. Composite Structures 2010; 92:1176-1183.
[19] Kharazi M, Oversy H R, Mooneghi M. Buckling analysis of delaminated composite plates using a novel layerwise theory. Thin-Walled Structures 2014; 74:246-254.
[20] Suemasu H, Kumagai T, Gozu K. Compressive behavior of multiply delaminated composite laminates part 1: experiment and analytical development. AIAA Journal 1998; 36(7):1279-1285.
[21] Stone M A, Chandler H D. Errors in double sine series solutions for simply supported symmetrically laminated plates. International Journal of Mechanical Sciences 1996;38(5):517–26.
[22] Tang Y, Wang X. Buckling of symmetrically laminated rectangular plates under parabolic edge compressions. International Journal of Mechanical Sciences 2011;53(2):91–7.
[23] Wu Z, Raju G, Weaver P M. Postbuckling analysis of variable angle tow composite plates. International Journal of Solids and Structures 2013; 50:1770-1780.
[24] Diaconu C G, Weaver P M. Approximate solution and optimum design of compression-loaded postbuckled laminated composite plates. AIAA Journal 2005; 43(4), 906–914.
[25] Davidson B D. Delamination buckling : theory and experiment. Journal of Composite Materials 1991; 25:1351-1378.